Biology of Blood and Marrow Transplantation 8:175-187 (2002)

Pulmonary Irradiation-Induced Expression of VCAM-1 and ICAM-1 Is Decreased by Manganese Superoxide Dismutase–Plasmid/Liposome (MnSOD-PL) Gene Therapy

Michael W. Epperly,[1] Christine A. Sikora,[1] Stacy J. DeFilippi,[1] Joan E. Gretton,[1] Dafna Bar-Sagi,[3] Herbert Archer,[3] Timothy Carlos,[2] HongLiang Guo,[1] Joel S. Greenberger[1]

[1]Department of Radiation Oncology, University of Pittsburgh Cancer Institute, Pittsburgh, Pennsylvania; [2]Department of Medicine, Division of Hematology/Oncology, University of Pittsburgh Medical Center, Pittsburgh, Pennsylvania; [3]Department of Molecular Genetics and Microbiology, State University of New York at Stonybrook, Stonybrook, New York

Correspondence and reprint requests: Joel S. Greenberger, MD, Professor and Chairman, Department of Radiation Oncology, University of Pittsburgh School of Medicine, 200 Lothrop St, Room B346-PUH, Pittsburgh, PA 15213 (e-mail: greenbergerjs@msx.upmc.edu).

Received April 24, 2001; accepted January 11, 2002

ABSTRACT

Pulmonary toxicity is a major complication of total body irradiation used in preparation of patients for bone marrow transplantation. The mechanism of the late pulmonary damage manifested by fibrosis is unknown. In C57BL/6NHsd mice, manganese superoxide dismutase–plasmid/liposome (MnSOD-PL) intratracheal injection 24 hours prior to 20 Gy single-fraction irradiation to both lungs significantly reduced late irradiation damage. Single intratracheal injections of MnSOD-PL, at concentrations as low as 250 μg of plasmid DNA, in a constant volume of 78 μL of liposomes, reduced late damage. To determine whether a slowly proliferating population of cells in the lung was responsible for initiation of fibrosis and was altered by MnSOD-PL therapy, 20 Gy total lung–irradiated mice were examined at serial time points for bromodeoxyuridine (BrdU) uptake in sites of cell division. There was low-level, but nonsignificant, increased cell proliferation detected at 80 days, with a significant increase at 100 days, 120 days, and at the time of death. Immunohistochemical assay for up-regulation of adhesion molecules associated with recruitment, transendothelial migration, and proliferation of bronchoalveolar macrophages revealed significant up-regulation of vascular cell adhesion molecule-1 (VCAM-1) and intracellular adhesion molecule-1 (ICAM-1) at 100 days with further increases up to the time of death. Increases were first detected in endothelin-positive endothelial cells. MnSOD-PL administration prior to irradiation decreased both BrdU incorporation and delayed expression of VCAM-1 and ICAM-1. The data indicate that the appearance of late irradiation-induced pulmonary fibrosis is associated with the up-regulation of adhesion molecules and suggest that potential targets for intervention may focus on the pulmonary vascular endothelium.

KEY WORDS

MnSOD-PL • Pulmonary fibrosis • Total body irradiation

INTRODUCTION

A major complication of total body irradiation (TBI) used in preparing patients for bone marrow transplantation (BMT) is pulmonary toxicity [1-12]. Despite the use of fractionated irradiation, transmission blocks for attenuation of dose, and reduced irradiation dose-rate, pulmonary toxicity remains a major clinical problem in TBI [8,11-14]. Radiation pulmonary damage is associated with an initial acute reaction of pneumonitis, in which bronchoalveolar and endothelial cellular swelling is associated with significant alveolar transudates and accumulation of inflammatory cells [8-9,15-24]. Acute reactions are often treated with nonsteroidal antiinflammatory agents, but may require administration of corticosteroids, the withdrawal of which can be problematic because of the recurrence of pathophysiological sequelae [10-12,25]. A subpopulation of patients recovering from acute radiation pneumonitis, as well as another subgroup not developing the acute reaction, will develop a late

Dr. Joel S. Greenberger is a member of the Scientific Advisory Board of Automated Cell, Inc, located in Oakmont, Pa, and is a holder of equity in the company.

picture of irradiation fibrosis [8]. Fibrosis has been associated with the detection of increased levels of collagen deposition and elaboration of transforming growth factor β1 (TGFβ1) and TGFβ2 and other cytokines [26-36]. The molecular mechanism(s) and cellular events associated with initiation of the late irradiation-induced pulmonary lesion are not known.

In C57BL/6NHsd mice receiving 20 Gy single-fraction total lung irradiation, the pathophysiological events associated with acute and chronic pulmonary irradiation damage are similar to those in the human [37-43]. In particular, late irradiation fibrosis, termed organizing alveolitis in the mouse model, is characterized by the proliferation of fibroblasts in the periphery of the lung at approximately 100 days after irradiation [43]. These lesions progress over the next 20 to 50 days and are associated with significant respiratory compromise and death [42-43].

We have previously demonstrated that intratracheal (IT) injection of manganese superoxide dismutase–plasmid/liposome (MnSOD-PL) prior to irradiation significantly reduces the extent and severity of organizing alveolitis in C57BL/6NHsd mice and improves survival [37-41]. Previous studies demonstrated that MnSOD-PL administration prior to irradiation reduced the second peak of elevation in levels of TGFβ1-β2 messenger RNA detected in lung specimens removed at days 100 and 120 after irradiation up to the time of death [38]. The cellular and molecular mechanisms of the late elevation in levels of TGFβ1-β2 are not known. One hypothesis to explain the late elevation in transcription of TGFβ1-β2 and the initiation of organizing alveolitis/fibrosis is that a slowly proliferating population of cells in the lung with a latent period of 100 days initiates the process of late irradiation damage [8]. A second hypothesis is that inflammatory cells, including bronchoalveolar macrophages (BAMs), are recruited to sites of irradiation injury by up-regulation of specific adhesion molecules that reach a critical threshold for signaling subsequent events [34-36,44-48].

In the present studies, after administering 20 Gy irradiation, we used the bromodeoxyuridine (BrdU) labeling technique to examine the lungs of C57BL/6NHsd mice at multiple time points for the detection of a slowly proliferating cell population in the endothelial or bronchoalveolar compartment. We also tested whether adhesion molecules known to be associated with inflammatory cell migration and proliferation might be up-regulated at the 100-day late time point. Initiation of late irradiation damage was decreased by IT injection of MnSOD-PL (in constant volumes of 78 μL) in plasmid DNA concentrations as low as 250 μg prior to delivery of 20 Gy single-fraction irradiation. The results demonstrate that MnSOD-PL administration modifies the increase in BrdU uptake by both macrophages and fibroblasts and increases VCAM-1 and ICAM-1 expression in endothelin-positive endothelial cells that are detected in areas of developing organizing alveolitis/fibrosis at approximately day 100 after pulmonary irradiation.

MATERIALS AND METHODS

Mice, Irradiation, and Histopathology

In the present studies, C57BL/6NHsd mice (Harlan Sprague Dawley, Indianapolis, IN) were used, whereas in prior studies, we have used C57BL/6J mice (both strains were obtained from Jackson Laboratories, Bar Harbor, ME). C57BL/6NHsd female mice (body wt, 25-30 g) were injected IT or intravenously (IV) with MnSOD-PL or bacterial β-galactosidase gene–plasmid/liposome (LacZ-PL) at 0 to 500 μg of plasmid DNA and received 20 Gy irradiation 24 hours later to both lungs using a Varian 600C Linear Accelerator (Varian Medical Systems, Palo Alto, CA). The mice were shielded so that only the pulmonary cavity was irradiated. The mice were watched on a daily basis for development of pulmonary fibrosis. Other mice received liposomes, but not plasmid. The mice were sacrificed at varying time points, lungs were excised, and 5 sections (each 10 microns thick) of each of 5 lobes were prepared using a Shandon AS620E Cryotome (Shandon/Lipshaw, Pittsburgh, PA). The sections were hematoxylin-eosin stained according to published methods [41].

Construction and Use of a Hemagglutinin Epitope–Tagged MnSOD

A hemagglutinin (HA) epitope–tagged MnSOD transgene was constructed that maintained biochemical activity. The HA tag was present in the pCGN vector prior to cloning in the MnSOD gene. The HA tag was located downstream of the cytomegalovirus (CMV) promoter and is upstream of the multiple cloning site. The MnSOD sequence was inserted into that vector using a 5′ XbaI site and a 3′ KpnI site located in the multiple cloning site and present on the MnSOD gene as part of the polymerase chain reaction primers. The protein product, therefore, contained an N-terminal HA tag, followed by the mitochondrial localization sequence (intrinsic to the coding sequence), followed by the mature protein at the C-terminal end. C57BL/6NHsd female and other mice (body wt, 25-30 g) were injected IT or IV with HA-epitope–tagged MnSOD-PL consisting of 500 μg of HA-MnSOD-PL in 50 μL of plasmid DNA complexed with 28 μL of lipofectant. The mice were anesthetized with Nembutal, the trachea was surgically exposed, and a 28-gauge needle was used to inject HA-MnSOD-PL into the trachea. IV injection of HA-MnSOD-PL was performed via the tail vein. The mice were sacrificed 24 hours later. The lungs were expanded in Optimum Temperature Cutting (OCT) compound (Sakura Fine Tek, Torrance, CA), excised, frozen in OCT, and sectioned. The sections were examined for expression of the HA-MnSOD-PL transgene, as described below, using an antibody against the HA epitope. Fluoroscein isothiocyanate (FITC)-monoclonal anti-HA antibody was used to detect HA-MnSOD-PL in the experimental lung sections. Epitope-tagged HA-MnSOD-PL was prepared and IT injected, as was the pRK5-MnSOD preparation, according to published methods [41]. The biochemical activity of HA-MnSOD-PL was tested in vitro using a cell line prepared from adult C57BL/6NHsd mouse lung cells according to published methods [41,49]. The experiments were performed twice in triplicate. The cells are referred to as tracheal-bronchial cells, because they originated from either the trachea or bronchus.

BrdU Labeling of Lung Cell Division

Control mice and mice injected with MnSOD-PL 24 hours earlier were irradiated to 20 Gy. At times ranging from 0 to the time of death, mice were injected intraperitoneally

with 50 mg/kg of BrdU. The mice were sacrificed 1 hour later, and the lungs were then expanded with OCT, excised, frozen in OCT, sectioned, and immunohistochemically stained using a BrdU IHC System staining kit (Oncogene Research Products, Boston, MA). The sections were fixed by incubation in methanol for 30 minutes at 4°C, followed by incubation in 3% hydrogen peroxide (H_2O_2) in methanol and incubation of the sections in denaturing solution at room temperature for 30 minutes. Nonspecific binding was blocked by incubating the sections in 3% goat serum. The sections were then incubated with a biotinylated mouse anti-BrdU antibody (Oncogene Research Products) for 30 minutes and washed with phosphate buffered saline (PBS). Peroxidase-conjugated streptavidin was added, and the sections were incubated for 10 minutes, then washed with PBS. A diaminobenzedine mixture (Oncogene Research Products) was added to the sections, which were then incubated in the dark for 2 to 3 minutes, washed, and stained with hematoxylin, covered with Histomount (Oncogene Research Products), coverslipped, and examined microscopically.

Quantitative Immunohistochemical Detection of VCAM-1, ICAM-1, Platelet-Selectin, and Erythrocyte-Selectin

Control mice and mice injected with MnSOD-PL were sacrificed at time points ranging from 0 to the time of death after 20 Gy irradiation; the lungs were then expanded with OCT, excised, frozen, and sectioned. The sections were stained using murine antibodies against VCAM-1 (Pharmingen 01811D; Pharmingen, San Diego, CA), erythrocyte (E)-selectin (Pharmingen 09521D), platelet (P)-selectin (Pharmingen 09481D), or ICAM-1 (Seikagaku America, Falmouth, MA); the sections were fixed in methanol, incubated in 1% H_2O_2 for 2 minutes at room temperature, and washed in PBS. Nonspecific binding was blocked by incubating the sections in 2% goat serum for 3 minutes at room temperature. The primary antibodies were diluted 1:50 and placed on the tissue sections for 2 hours in a humidity box. The slides were washed in PBS, and a biotinylated antirat antibody was added to the sections. The sections were then incubated for 30 minutes at room temperature, followed by incubation with an avidin peroxidase macromolecular complex for 1 hour and washing in PBS. An amino-ethylcarbazole reagent (600 mg 3-amino-9-ethylcarbazole in 10 mL of N,N-dimethylformamide mixed with 100 mL of 0.02 mol/L sodium acetate, pH 5.2, plus 100 mL H_2O_2 solution)/formamide solution was then placed on the sections, and they were incubated for 10 minutes. The slides were washed in PBS, stained with hematoxylin for 2 minutes, and washed in water. The slides were mounted with antifade Histomount and coverslipped.

To both demonstrate and quantitate endothelial cell expression of ICAM-1 and VCAM-1 following irradiation to the lung, lung sections were costained with FITC-conjugated antibody to either ICAM-1 (hamster) or VCAM-1 (murine) and a rabbit antibody to endothelin (endothelin [Ab-2] polyclonal [catalog no. PC266, lot no. D14892], Oncogene Research Products) complexed with a phycoerythrin (PE)-conjugated goat antirabbit immunoglobulin G antibody (Oncogene Research Products). To determine the best concentration of antiendothelin antibody to be used in staining, lung sections from nonirradiated and irradiated mice were stained with 1:50, 1:100, or 1:250 dilutions of antiendothelin antibody. The sections were then stained with a 1:100 dilution of PE-conjugated goat antirabbit antibody (to determine the endothelin-positive cells) and examined using a Nikon FXA epifluorescence differential-interference contrast (DIC) light microscope (Nikon, Melville, NY).

We scored positive cells in each of 10 sections, counting more than 1000 cells per section. To determine the optimal concentration of (hamster) anti–ICAM-1 or (murine) anti–VCAM-1, lung sections from nonirradiated mice or mice that received 20 Gy irradiation 120 days previously were stained with a 1:50, 1:100, or 1:250 dilution of FITC-conjugated anti–ICAM-1 or FITC-conjugated anti–VCAM-1. The slides were examined using a fluorescent microscope, and the percentage of 1000 cells expressing ICAM-1 or VCAM-1 in each of 10 sections were scored. The antibody concentration that gave the most consistent result with the least autofluorescence was selected, and then lung sections from mice given 0 or 20 Gy irradiation were fixed in methanol. We blocked nonspecific binding by incubating the cells in 2% goat serum, washing in PBS, incubating slides with a 1:100 dilution of either FITC-conjugated anti–ICAM-1 or FITC-conjugated anti–VCAM-1 and a 1:100 dilution of antiendothelin antibody for 2 hours at room temperature. The slides were mounted with antifade Histomount, coverslipped, and examined using a Nikon FXA epifluorescence DIC light microscope. PE-labeled (red) cells indicated endothelin positivity and the FITC-labeled (green) cells indicated ICAM-1 and VCAM-1 positivity. Percentages of endothelin-positive cells and the subset of ICAM-1– and VCAM-1–positive cells were calculated using a dual-filter cube to look at the green fluorescence (530 nm) and the red fluorescence (615 nm); at the same time, the percentage of cells that were both endothelin positive and VCAM-1 or ICAM-1 positive (yellow) was scored.

Pulmonary Endothelial Cell Culture

C57BL/6NHsd mice were sacrificed and the thoracic cavity was exposed. Lungs were perfused by injecting 5 mL of PBS through the left ventricle, removed, rinsed, minced, and incubated for 45 minutes at 37°C in serum-free Dulbecco's Modified Eagle's Medium (DMEM) containing 100 Units of collagenase per mL. Cells were passed through an 18-gauge needle and filtered through a 70-μm filter; 5 mL of cold DMEM was added to the cells, and the mixture was centrifuged for 5 minutes at 100 rpm. The supernatant was removed and the cells were resuspended in media containing an antiplatelet endothelial cell adhesion molecule (PECAM) monoclonal antibody attached to Dynabeads (Dynal Biotech, Oslo, Norway), incubated for 30 minutes at 4°C with gentle mixing, then incubated in a Dyna MPC Unit (Dynal Biotech) for 2 minutes. The supernatant was removed, the beads were washed 5 times in PBS, and the endothelial cells were digested from the beads by incubating the beads in 1 mL of trypsin/ethylenediaminetetracetic acid (EDTA) for 5 minutes at 37°C. The cells were washed, resuspended, and grown in DMEM containing 5 μg/mL insulin, 30 μg/mL endothelial cell growth supplement, 15% fetal bovine serum, 20 mmol/L N-[2-hydroxyethyl]piperazine-N-[2-ethanesulfonic acid] (HEPES), and 10 Units/mL heparin.

*Effect of Varying Doses of MnSOD-PL prior to 20 Gy Irradiation on the Mean Survival Time of C57BL/6NHsd Mice**

Treatment Groups	Mean No. of Days	P
20 Gy irradiation	137.6 ± 5.4	
20 Gy + LacZ-PL (250 μg)	138.8 ± 4.2	
20 Gy + LacZ-PL (50 μg)	140.9 ± 2.9	
20 Gy + MnSOD-PL (500 μg)	154.9 ± 4.7†	.015
20 Gy + MnSOD-PL (250 μg)	165.7 ± 6.0†	.009
20 Gy + MnSOD-PL (100 μg)	144.6 ± 1.9	
20 Gy + MnSOD-PL (50 μg)	152.4 ± 6.4	

*C57BL/6NHsd mice were intratracheally injected with doses of MnSOD-PL or LacZ-PL (50-500 μg of DNA). Twenty-four hours later, control mice as well as mice injected with MnSOD-PL or LacZ-PL were irradiated to a dose of 20 Gy to the pulmonary cavity. The mice were followed for development of organizing alveolitis or fibrosis, as indicated by a loss of weight and difficulty in breathing, at which time the mice were sacrificed. The mean survival time was calculated and is shown with standard error of the mean. A Student *t* test was used to compare the mean survival time for the different groups.

†Only the mice injected with MnSOD-PL at 500-μg or 250-μg doses demonstrated significantly increased survival times compared to the groups receiving 20 Gy only, 250 μg of LacZ-PL, or 50 μg of LacZ-PL.

The endothelial cells were transferred to 4-chambered microscope slides and transfected with the HA-MnSOD plasmid using lipofectant by mixing 10 μg of plasmid DNA with 20 μg of lipofectant in a total volume of 200 μL of serum-free RPMI 1640 medium and incubating for 30 minutes at 37°C. The endothelial cells were washed twice with PBS. The DNA/liposome complex was diluted to 1 mL of serum-free RPMI 1640 medium, and 200 μL was added to each chamber. The cells were incubated at 37°C for 5 hours, at which time the cells were washed with PBS and 400 μL of RPMI 1640 medium containing 10% fetal calf serum. In other chambers, cells were treated in the same manner, except the liposomes contained no plasmid DNA. The chambers were irradiated to 20 Gy 24 hours later and stained for expression of VCAM-1, ICAM-1, P-selectin, or E-selectin, as described above, 24 hours after irradiation.

Statistics

Analysis of survival data comparing control irradiated mice and LacZ-PL–injected mice with the different MnSOD-PL groups was performed using a function called Survdiff using inverse Wilcoxon paired comparisons [50-51]. A Student *t* test [52,53] as part of GraphPad's Prism Statistical Analysis Program (GraphPad Software, San Diego, CA) was used to analyze the data comparing different irradiation groups with control or MnSOD-PL–injected mice.

Animal Welfare

The Institutional Animal Care and Use Committee of the University of Pittsburgh approved all protocols. The Central Animal Facility of the University of Pittsburgh provided veterinary care in strict accordance with the Institutional Animal Care and Use Committee of the University of Pittsburgh guidelines. The mice were housed in specific pathogen-free conditions in the presence of sentinel mice that were monitored once a month for pathogens. All sentinel mice were negative for all pathogens tested, in particular for those that cause pneumonitis.

RESULTS

Dose Levels of MnSOD Plasmid DNA in Plasmid/Liposomes Required to Increase Survival of C57BL/6NHsd Mice Irradiated to 20 Gy

To determine the dose of MnSOD plasmid DNA in a constant volume of 78 μL of plasmid/liposomes required to prevent late irradiation pulmonary damage, groups of C57BL/6NHsd female mice (body wt, 25-30 g) were injected IT 1 day prior to irradiation with doses of 500, 250, 100, or 50 μg of MnSOD plasmid DNA. The mice each received 20 Gy irradiation to both lungs and were followed for morbidity and significant pulmonary damage as detected by loss of weight and difficulty in breathing. Control animals receiving 250, 50, or 0 μg of LacZ plasmid DNA prior to irradiation had mean survival times of 138.8 ± 4.2, 140.9 ± 2.9, and 137.6 ± 5.4 days after irradiation, respectively (Table). In contrast, mice that received MnSOD-PL at plasmid DNA concentrations of 50 μg (survival, 152.4 ± 6.4 days) or 100 μg (survival, 144.6 ± 1.9 days) showed improvement in survival times, with statistically significant improvement occurring in groups receiving 250 μg or 500 μg (Table). These results confirm and extend our prior results of MnSOD-PL administration prior to radiation and show a protective effect at a 2-fold lower plasmid DNA dose compared to that reported in previous publications [37-41,54]. The results also establish the similarity of the pathologic sequelae of pulmonary irradiation between C57BL/6J and C57BL/6NHsd mice.

Identification of Cellular Sites of Uptake of MnSOD-PL Using an HA Epitope–Tagged Construct

Considering the detectable effect of relatively low doses (50 μg) of MnSOD DNA providing protection to the lung from irradiation, we performed studies to determine which cells were transfected by IT injection of MnSOD-PL and how delivery of IT injections compared to that of IV injections of MnSOD-PL. It was reasoned that endothelial cells might be less effectively transfected by the IT compared to the IV route, perhaps allowing us to target further studies to a specific cell population. To facilitate targeting and analysis of MnSOD-PL delivery to specific cells within the airway and bronchoalveolar lavage cells, we have used an HA-epitope–tagged construct, HA-MnSOD (Figure 1).

The biological effectiveness of the epitope-tagged HA-MnSOD-PL construct was demonstrated in an in vitro colorimetric assay measuring the reduction of nitro blue tetrazolium (NBT) by superoxides. C57BL/6NHsd mouse tracheal-bronchial cells transfected with HA-MnSOD-PL demonstrated a significant increase (P = .0015) in MnSOD biochemical activity of 6.7 ± 0.29 units of MnSOD activity per 1 mg of protein compared with 3.9 ± 0.41 units of MnSOD activity per 1 mg of protein for control tracheal-bronchial cells, as detected using our assay specific for MnSOD biochemical activity in 2 experiments performed in triplicate.

In previous studies, it was difficult to determine which cells were transfected following IT injection of MnSOD-PL. Using HA-MnSOD-PL, we determined which cells

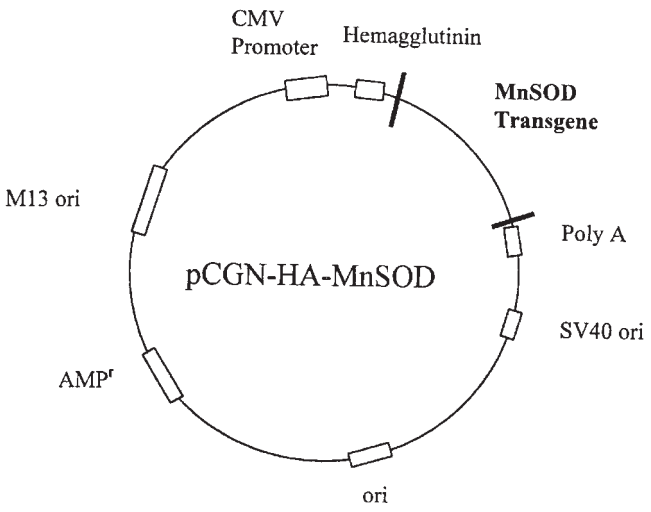

Figure 1. Hemagglutinin (HA) epitope–tagged MnSOD construct (pCGN-HA-MnSOD).

expressed HA-MnSOD and whether IT or IV injections provided similar delivery to endothelial compared to alveolar type II bronchoalveolar cells (Figure 2). Mice were IV or IT injected with 500 μg of HA-MnSOD plasmid DNA in 78 μL of plasmid/liposomes. Upon examination of lung sections stained with an anti-HA antibody and an antiendothelin antibody, endothelial cells showed HA-MnSOD expression (>50%) 24 hours following either route of injection (Figure 2). In contrast, the noninjected mice demonstrated negative reactivity with the antibody to HA (Figure 2). Thus, IV or IT injection of HA-MnSOD-PL resulted in significant plasmid uptake in endothelial cells. There was also detectable HA-MnSOD expression in bronchoalveolar cells by the IT route of administration.

Detection of Significant Proliferation of Bronchoalveolar Cells in the Periphery of the Lung at 100 Days after 20 Gy Single-Fraction Irradiation

To determine whether initiation of the late organizing alveolitis (fibrosis) pulmonary lesion was associated with a

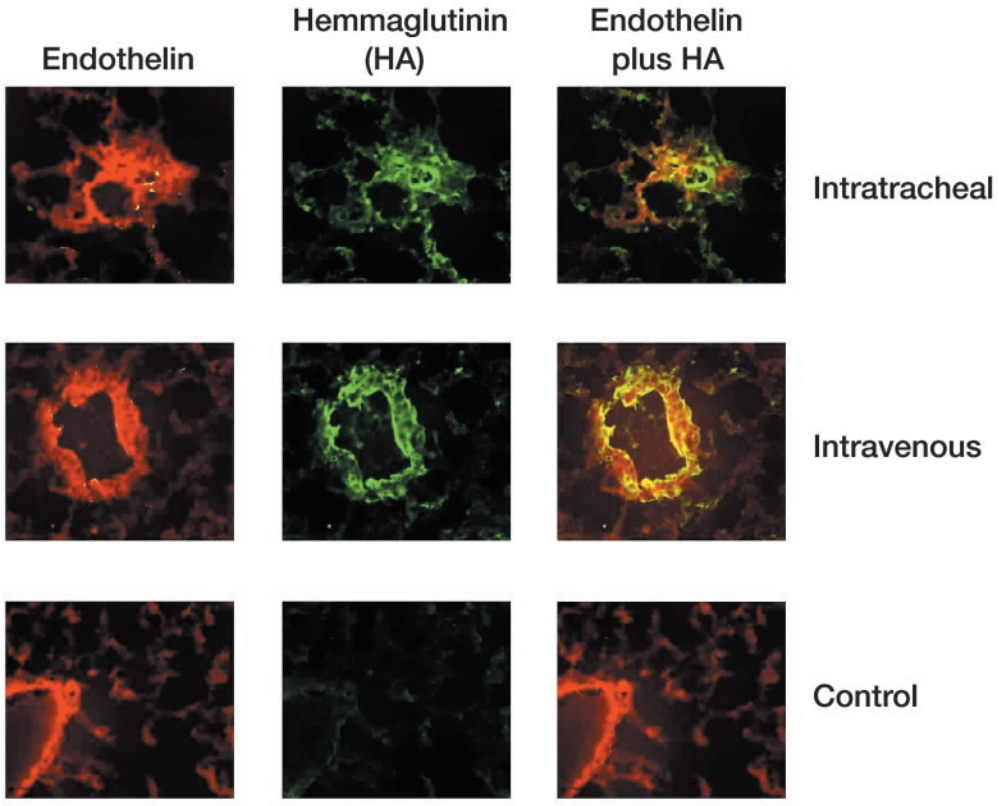

Figure 2. Fluorochrome antibody (antihemagglutinin [HA]) detection of plasmid HA-MnSOD in the endothelial cells of C57BL/6J mouse lungs 24 hours after intratracheal or intravenous injection of plasmid/liposomes. Mice were injected either intratracheally or intravenously with HA-MnSOD–plasmid/liposome and sacrificed 24 hours later; the lungs were then excised, frozen in OCT compound, and sectioned. The sections were costained with an FITC-conjugated antibody to HA and a rabbit antiendothelin antibody, followed with PE-conjugated goat antirabbit antibody. The sections were examined using a fluorescent microscope. The top row panel is from a mouse injected intratracheally, whereas the middle row panel is from a mouse injected intravenously. The bottom row panel is from a control noninjected mouse. The first column shows fluorescence from the PE-labeled (red) endothelin-positive cells, whereas the middle column demonstrates the FITC-labeled (green) HA-positive cells. The third column displays the fluorescence from both fluorochromes, with the yellow color representing cells positive for both endothelin and HA. Intratracheal injections resulted in HA expression in endothelial cells as well as in alveolar cells, whereas intravenous injections demonstrated HA expression in only the endothelial cells (original magnification ×1000).

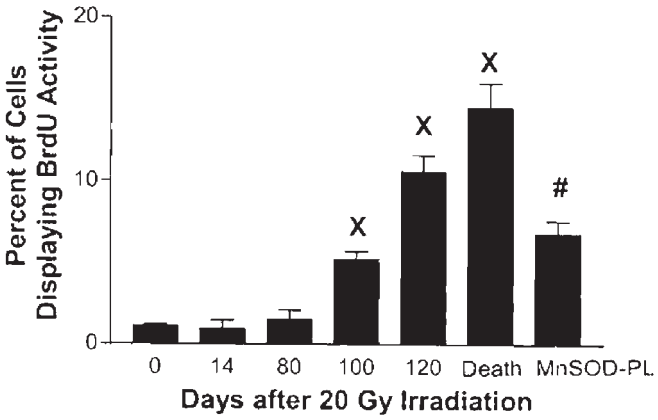

Figure 3. Detection of increased BrdU uptake in irradiated C57BL/6J mouse lungs. MnSOD-PL–injected or control C57BL/6J mice were irradiated to 20 Gy to the pulmonary cavity. At days 0, 14, 80, 100, or 120, or immediately prior to death, the control mice were injected with 50 mg/kg BrdU and sacrificed 1 hour later. MnSOD-PL mice were injected with BrdU on the same day as the control mice and were sacrificed 1 hour later. The lungs were expanded with OCT, excised, frozen in OCT, and sectioned. The sections were stained for BrdU uptake using an anti-BrdU antibody and examined microscopically for the percentage of cells showing BrdU uptake (scoring 1000 cells in 5 sections from each of 5 lobes of at least 3 mice per point) (compared to control nonirradiated lung at days 100 or 120 or immediately prior to death [indicated by X], $P < .05$). Mice that were injected with MnSOD-PL and then irradiated had a significantly lower level of BrdU incorporation than did the control irradiated mice immediately prior to death (indicated by #).

slowly proliferating population of cells, mice were sacrificed at days 0, 14, 80, 100, or 120 or at the time of premorbid condition prior to death after receiving 20 Gy total lung irradiation, and the lungs were examined for uptake of BrdU. In other groups, mice injected with MnSOD-PL and irradiated to 20 Gy were sacrificed at the same time as the premorbid mice. The premorbid irradiated control group demonstrated signs of pulmonary distress, such as difficulty in breathing, lack of movement, and weight loss, whereas the MnSOD-PL–treated mice were asymptomatic. The explanted pulmonary sections were fixed (as described in "Materials and Methods") and assayed for immunohistochemically detectable BrdU. As shown in Figure 3, there was a low-level, but detectable, increase in cell proliferation in control irradiated mice at day 80 (Figure 4B); however, this level did not reach statistical significance above that of the pretreatment groups. In contrast, by day 100, there was significant increase in uptake of BrdU that was localized to peripheral areas in the lung adjacent to the pleural walls (Figure 4C), the area where organizing alveolitis and fibrosis develop. By day 120 or prior to death, there was a significant further increase in BrdU uptake in areas that were localized immunohistochemically to the peripheral lung areas (adjacent to visceral pleura) associated with developing fibrosis (Figure 4D). Irradiated mice injected with MnSOD-PL and killed at the same time as the mice in Figure 4D had less BrdU incorporation (Figures 3 and 4E). Examination of endothelial cells by antiendothelin stain in these sections failed to detect significant BrdU uptake in endothelial cells under conditions in which increased macrophage and fibroblast BrdU uptake was observed.

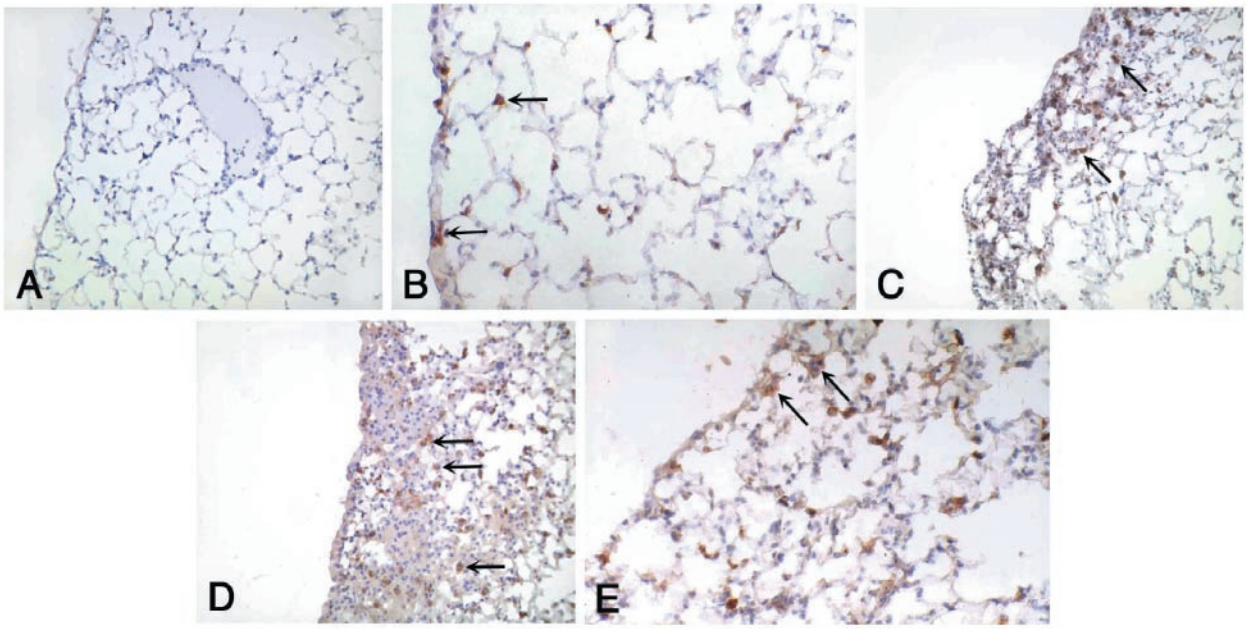

Figure 4. Demonstration of BrdU-positive mitotic cells within an area of pulmonary fibrosis. Representative specimens from time points from Figure 3 at: day 0 (A), day 80 after 20 Gy irradiation (B), day 100 after 20 Gy irradiation (C), prior to death (D), or MnSOD-PL–treated mice at the time of death of the control irradiated mice (E). Arrows show positive areas by anti-BrdU immunohistochemical staining at the periphery of the lung in areas initiating near the visceral pleura. There was significantly less BrdU incorporation in MnSOD-PL–treated irradiated lung (E) compared to that in control irradiated lung (D) immediately prior to death (A, C, and D, original magnification ×100; B and E, original magnification ×200).

Correlation of BrdU-Uptake Sites to Microscopic Sites of Increase in VCAM-1 and ICAM-1 at 80 Days after 20 Gy Single-Fraction Lung Irradiation

We next investigated whether there was an immunohistochemically detectable increase in a specific adhesion molecule in the lungs, specifically at the peripheral lung areas that showed increased BrdU uptake, and whether this increase occurred at time points prior to BrdU-detectable increased cell proliferation. MnSOD-PL–injected mice and control mice were irradiated to 20 Gy, sacrificed at days 0, 14, 80, 100, or 120 or when moribund prior to death, and examined immunohistochemically for detection of E-selectin, P-selectin, ICAM-1, and VCAM-1. At 80 days after irradiation, there was a small increase detected in VCAM-1 and ICAM-1 levels, but not in E-selectin or P-selectin, in irradiated mice (Figure 5). The increases were detected in the peripheral subpleural areas of lung and also in other areas in a patchy nonuniform pattern. Thus, the evidence suggested that the initiating events in late fibrosis were associated with both adhesion molecule up-regulation in endothelial cells at the time of detectable fibroblasts and macrophage cell proliferation in areas of developing organizing alveolitis/fibrosis.

As shown in Figure 5, there were significant increases in expression of ICAM-1 and VCAM-1 beginning at 100 days after 20 Gy total lung irradiation in the control irradiated mice compared to that in the MnSOD-PL–pretreated mice or nonirradiated mice ($P < .0001$ and $P < .0001$, respectively). The increases in ICAM-1 and VCAM-1 expression in the control irradiated mice compared to the nonirradiated mice persisted and increased further by day 120; these increases were also significantly greater immediately prior to death (Figure 5). In mice injected with MnSOD-PL prior to irradiation, increased expression of ICAM-1 and VCAM-1 was not detected until day 120 (Figure 5). There were no detectable increases in levels of expression of E-selectin or P-selectin in any of the mice.

The sites of increased expression of VCAM-1 and ICAM-1 were critically examined in explanted lung samples. There was a significant increase in ICAM-1 in whole lung cells at 100 days in the control irradiated mice, but not in MnSOD-PL–pretreated mice. There was an increase in expression of ICAM-1 and VCAM-1 in control irradiated mice at 120 days (Figure 5). There was an increase in VCAM-1 at day 100 in control irradiated mice compared to that in MnSOD-PL–pretreated mice, and expression of both ICAM-1 and VCAM-1 was further increased in control irradiated mice at day 120 (Figure 5). The ICAM-1 and VCAM-1 elevations were next evaluated by immunofluorescence staining to determine whether endothelial cells were identifiable. The up-regulation was evaluated in the 120-day sections and was localized predominantly to endothelial cells as demonstrated by costaining the lung sections with FITC-conjugated antibodies to either ICAM-1 or VCAM-1 and PE-conjugated goat antirabbit antiendothelin antibody.

To quantitatively determine which dilution of antibody resulted in the least autofluorescence while presenting maximal positive staining, lung sections were stained with different dilutions of a rabbit antiendothelin antibody and a constant PE-conjugated goat antirabbit antibody (Figure 6A), FITC-conjugated anti–ICAM-1 (Figure 6B), or FITC-conjugated anti–VCAM-1 (Figure 6C). For all 3 antibodies, a 1:100 dilution provided the optimal staining for PE or FITC with the lowest background level of autofluorescence.

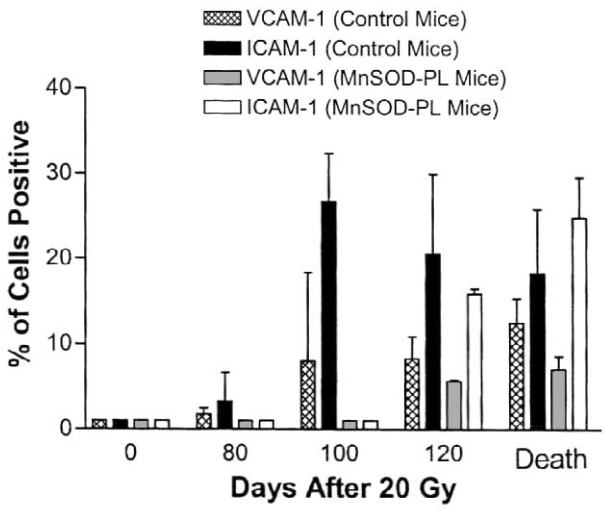

Figure 5. Expression of VCAM-1, ICAM-1, P-selectin, and E-selectin in mouse lungs after irradiation. Control C57BL/6J mice or mice injected with MnSOD-PL were irradiated to 20 Gy to the pulmonary cavity and sacrificed on days 0, 80, 100, or 120 or at the time of death. The lungs were frozen in OCT compound, sectioned, and then stained by immunohistochemistry as described in "Materials and Methods." The sections were examined microscopically, and the percentage of cells expressing the adhesion molecules was determined. There was a significant increase in expression of VCAM-1 and ICAM-1 beginning at 100 days after irradiation for control irradiated mice compared to that of nonirradiated mice ($P < .0001$) or irradiated MnSOD-PL–treated mice 100 days after irradiation ($P < .0001$) (1000 cells scored in 5 slides from each of 5 lobes; 3 mice per point). The increase in ICAM-1 and VCAM-1 expression was delayed in MnSOD-PL–treated mice until 120 days after irradiation.

The percentage of endothelin-positive cells at 120 days was similar in control nonirradiated and 20 Gy–irradiated lungs at each dilution of antibody (Figure 6A). Thus, irradiation did not alter the antiendothelin-positive cell number per lung section. In contrast, irradiated lung sections showed a higher percentage of ICAM-1– and VCAM-1–positive, endothelin-positive cells at 1:50 and 1:100 dilutions of antibodies (Figures 6B and 6C). To confirm that the irradiation-induced increased ICAM-1 and VCAM-1 expression observed by immunohistochemistry in whole lung was in anatomically localized endothelial cells, lung sections were costained with mouse FITC-conjugated antibodies to either ICAM-1 or VCAM-1 and a rabbit antiendothelin antibody. The sections were then stained with a PE-conjugated goat antirabbit antibody, which could detect the endothelin-positive cells. Increased ICAM-1 (Figure 7A) and VCAM-1 (Figure 7B) expression was clearly associated with endothelin-positive cells. The data demonstrate that the increased expression of ICAM-1 and VCAM-1 in irradiated lung sections at 120 days was in endothelial cells.

To determine whether the histochemically VCAM-1–positive cells detected in vivo were similar in staining to in vitro cultured endothelial cells and whether an HA-

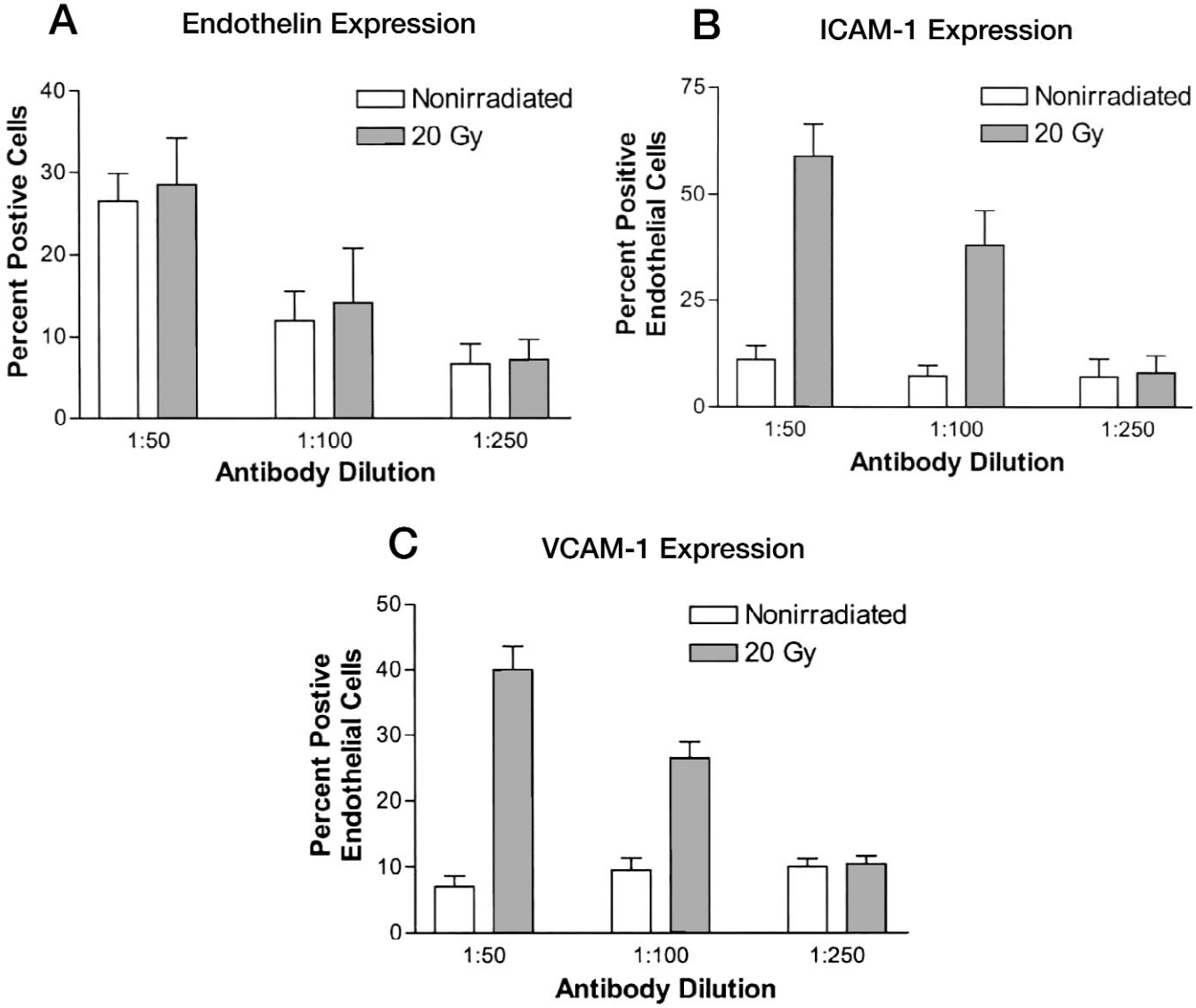

Figure 6. Dose-response curve for determination of antibody dilutions for costaining lung samples with anti–ICAM-1, anti–VCAM-1, and antiendothelin antibodies. Lung sections from nonirradiated mice and from mice irradiated to 20 Gy to the pulmonary cavity were explanted at day 120 and stained with each dilution of antibody to endothelin, ICAM-1, or VCAM-1, as described above. The sections were observed using a fluorescent microscope, and the percentages of cells positive for endothelin alone (A), ICAM-1 and endothelin (B), or VCAM-1 and endothelin (C) were determined. The optimal antibody dilution yielding the highest percentage of positive cells for endothelin alone (A), ICAM-1 plus endothelin (B), or VCAM-1 plus endothelin (C), but yielding the lowest autofluorescence, was a 1:100 dilution for all 3 primary antibodies (the goat antirabbit antibody was separately optimized at a 1:100 dilution; see "Materials and Methods").

MnSOD-PL effect was detectable in vitro, pulmonary endothelial cells were explanted from C57BL/6NHsd mouse lung to culture using techniques described in "Materials and Methods." One half of the cells were HA-MnSOD-PL–transfected in vitro, whereas the remaining half of the cells were transfected with LacZ-PL. The transfection procedure had no effect on the viability of the cells, with more than 95% of cells in each group viable following transfection. The endothelial cell cultures were irradiated in vitro to 20 Gy, then 24 hours later were immunohistochemically examined for detectable VCAM-1. Irradiation-induced VCAM-1 was detected in 29.4% ± 3.8% of the mock-transfected cells (Figure 8B). HA-MnSOD-PL transduction of endothelial cells in vitro prior to irradiation demonstrated a significant reduction in VCAM-1–positive endothelial cells (6.7% ± 1.5%, $P = .005$) (Figure 8C).

DISCUSSION

Pulmonary complications remain a major dose-limiting factor in the design of protocols for TBI in patients receiving BMT [11-14]. The acute effects of TBI with respect to lung complications have been associated with opportunistic infections, the interaction of acutely irradiated tissues with donor bone marrow in graft-versus-host disease, and cytokine release. TGFβ1-β2, interleukin-1 (IL-1), and tumor necrosis

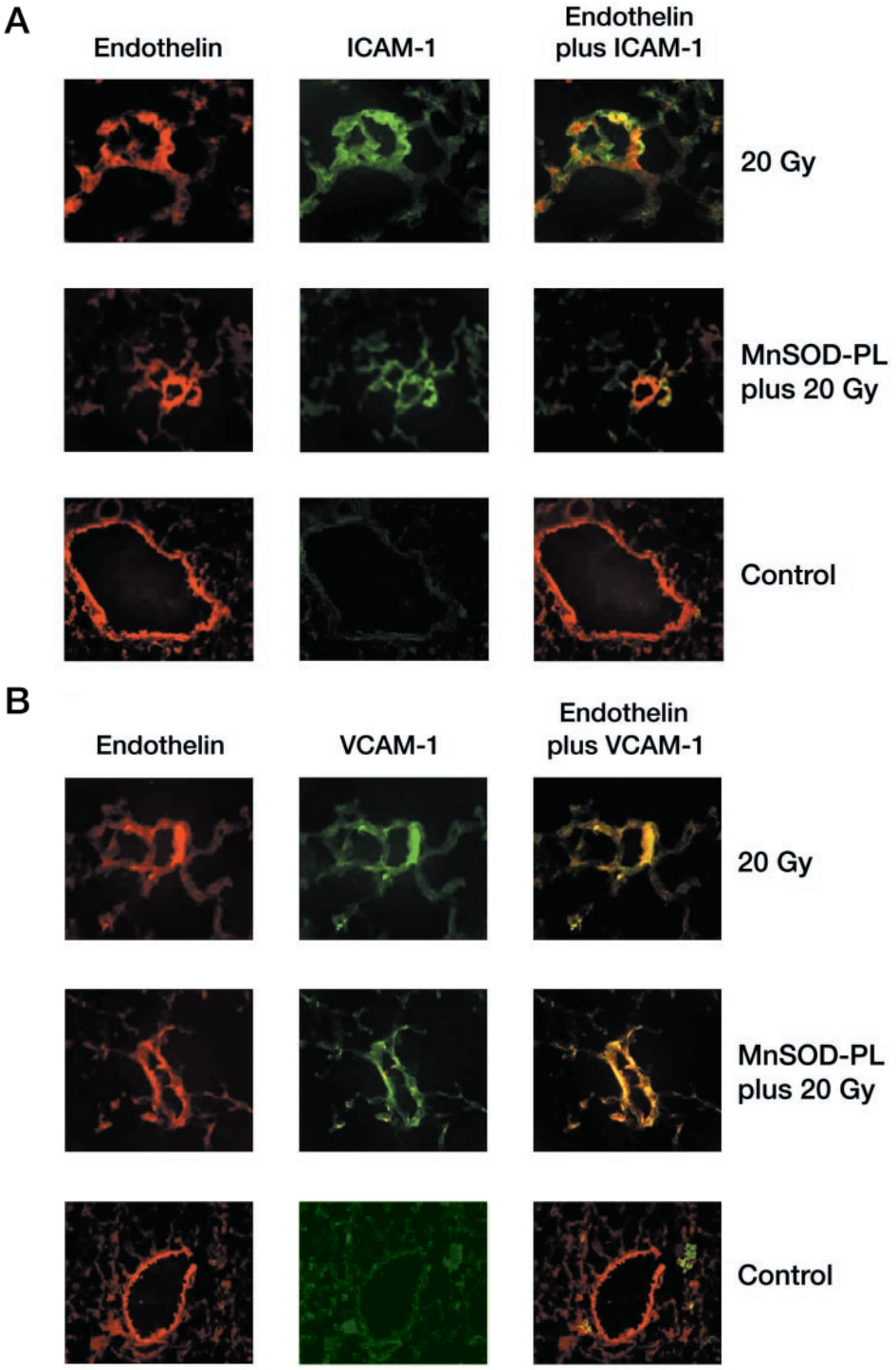

Figure 7. Increased ICAM-1 and VCAM-1 in pulmonary endothelial cells following irradiation. To demonstrate that increased ICAM-1 (A) and VCAM-1 (B) expression was in the endothelial cells, lung sections of C57BL/6J mice were costained with a rabbit antibody to endothelin and either hamster FITC-conjugated antibody to ICAM-1 (A) or murine FITC-conjugated anti–VCAM-1 (B). The sections were then stained with a PE-conjugated antirabbit antibody to detect endothelin-positive cells and examined using a fluorescent microscope. In A and B, the top row panel is representative of a lung section from a mouse that received 20 Gy irradiation 120 days previously. The middle row panel is a section from a mouse that received MnSOD-PL and 20 Gy irradiation at 120 days previously, whereas the bottom row panel is from a nonirradiated mouse. The first column is the fluorescence obtained from the PE-labeled anti–rabbit-endothelin antibody (red), whereas the second column is the emission from the FITC-labeled anti–ICAM-1 (green) (A) or FITC-labeled anti–VCAM-1 antibody (green) (B). The column on the right is the emission from both fluorochromes with the yellow color representing cells expressing both endothelin and either ICAM-1 or VCAM-1. Increased expression of ICAM-1 in endothelial cells is shown (A). Mice injected with MnSOD-PL before 20 Gy irradiation had decreased expression of ICAM-1 compared to the control irradiated mice. B, Increased expression of VCAM-1 in endothelial cells from control irradiated mice and MnSOD-PL–treated then irradiated mice (original magnification ×1000).

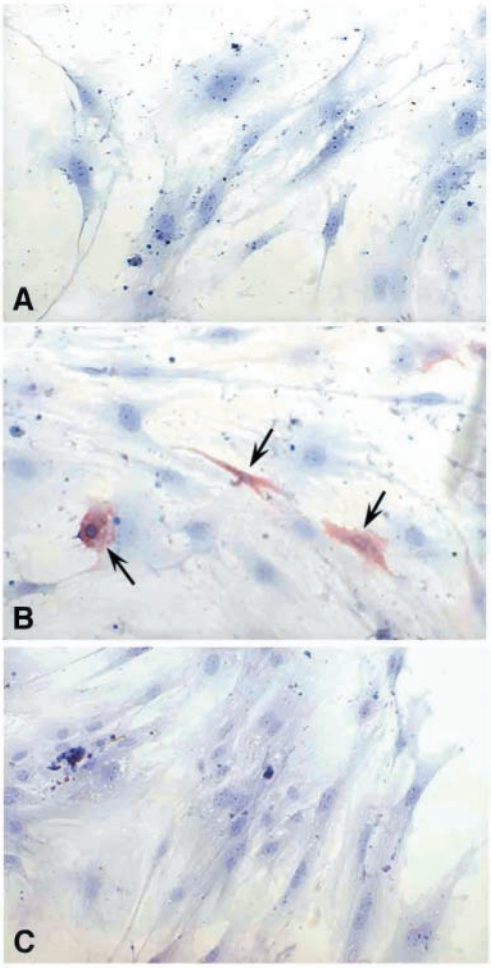

Figure 8. Increased VCAM-1 expression induced in C57BL/6NHsd mouse pulmonary endothelial cells in vitro by 20 Gy irradiation. Pulmonary endothelial cells were isolated as described in "Materials and Methods." Fifty percent of the cells were transfected with HA-MnSOD plasmid using lipofectant, whereas the remaining cells were either untreated or transfected with LacZ plasmid. The cells in each group were irradiated 24 hours later to 20 Gy and stained 24 hours later with anti–VCAM-1 antibody. Nonirradiated control endothelial cells (A) are shown compared to irradiated endothelial cells (B). HA-MnSOD-PL–transfected cells 24 hours prior to 20 Gy irradiation are shown (C). VCAM-1 expression (arrow) was significantly increased in irradiated control cells (B) compared to that in MnSOD-transfected cells (C). ICAM-1 expression was also increased following irradiation of endothelial cells, but was decreased in HA-MnSOD-PL–treated cells (original magnification ×1000).

factor-α (TNF-α) have been associated with irradiated lung volumes in TBI [26-30]. The use of fractionation regimens, transmission of lung blocks, and other shielding techniques have greatly reduced the acute toxicity of TBI-induced lung damage. However, reports of late recurrence of tumor associated with lung shielding techniques have suggested the possibility that reduced irradiation doses to the vertebral bodies and ribs in these shielded areas may compromise total marrow irradiation doses [12]. Late pulmonary irradiation damage in long-term survivors of TBI and BMT has provided a further impetus for research in understanding the radiation biology of lung damage [11-14].

We have previously demonstrated that 2 peaks of elevation in levels of TGFβ1-β2 occur in the C57BL/6J female mouse lung following total lung irradiation [38]. In the acute irradiation reaction (7-10 days after total lung irradiation), elevation of TGFβ1-β2 is associated with an elevation of TNF-α and IL-1 as well as other cytokines [38]. In the late irradiation reaction associated with organizing alveolitis/fibrosis, TNF-α elevation was observed to precede the late peak of TGFβ1-β2 [38]. This latter peak in elevation of TGFβ1-β2, but not the earlier increases in TNF-α and IL-1, was associated with proliferation of fibroblasts in the peripheral areas of the lung, as shown by the histopathological sequelae of organizing alveolitis [43]. In previous studies, we demonstrated that IT injection of MnSOD-PL reduced both the early and late peak elevations of cytokines and decreased the magnitude and severity of organizing alveolitis/fibrosis [38]. In the present studies, we sought to determine whether there was a MnSOD plasmid dose–dependent reduction in irradiation damage.

The present studies demonstrate that doses of MnSOD-PL, at concentrations as low as 250 μg of plasmid DNA, in a constant volume of 78 μL of plasmid/liposomes, were effective in reducing the toxicity of 20 Gy total lung irradiation. In other studies, lower doses of 10 μg and 1 μg were not detectably effective compared to irradiation alone.

The pathophysiological mechanism of late irradiation damage has remained a mystery in radiation biology. After the acute irradiation in the lung, cytokine messenger RNA and protein levels returned to baseline levels, the histopathological evidence of alveolar or endothelial cell swelling was absent, and the pulmonary function tests and other measures of pulmonary circulation all returned to normal. After an unexplained latent period, cytokine levels again were elevated, bronchoalveolar inflammatory cell infiltrates were detected, and there was a rapid onset in the mouse model showing a pattern of organizing alveolitis/fibrosis with proliferation of fibroblasts and obliteration of normal lung volume [13-14,38,55]. In the present studies, we sought to determine if one potential mechanism of this late effect could be explained by a slowly proliferating cell population requiring 100 days for expression of irradiation damage [8]. BrdU labeling studies detected low levels of cellular proliferation throughout the lung on day 80 and significant proliferation in the areas of initial organizing alveolitis/fibrosis at day 100, extending to day 120, and immediately prior to death. Proliferating cells were fibroblasts with significantly lower, but detectable, numbers of BAMs. There was no significant increase in proliferation of pulmonary endothelial cells. In contrast, experiments quantitating intracellular expression of VCAM-1 and ICAM-1, P-selectin, and E-selectin at the same time points demonstrated a distinctly different pattern of expression. Pulmonary cells in the total lung showed a significant increase in detectable VCAM-1 as early as day 80, with a significant, further increase up to days 100 and 120. There was also a significant increase in ICAM-1 in the periphery of the lung, which was the principal site of proliferation and detectable BrdU uptake. No significant increase in E-selectin or P-selectin expression was seen at any of these time points. Scoring of immunohistochemically positive cells using specific costain-

ing with both antiendothelin and anti–VCAM-1 or anti–ICAM-1 showed a higher positive percentage in endothelial cells in irradiated lung at 120 days than in whole lung. Thus, endothelial cells clearly were a large fraction of the VCAM-1– and ICAM-1–positive cell population detected at day 120 after 20 Gy irradiation of whole lung.

The evidence from these experiments suggests that up-regulation of VCAM-1 and ICAM-1 in endothelial cells occurs approximately 100 days after irradiation and may be one of the events in late irradiation-induced murine organizing alveolitis/fibrosis. To determine whether endothelial cells were detectably transduced by MnSOD-PL following IT injection (the method shown to be protective in our previous studies), we used an epitope-tagged HA-MnSOD-PL for injection. These studies showed that IT as well as IV injections of HA-MnSOD-PL demonstrated a significant uptake of the MnSOD construct in endothelial cells. Because this HA-MnSOD-PL construct was also biochemically active, the data suggest that the radioprotective effect of MnSOD-PL administration by IT injection could have been initiated through events in the endothelial cells.

Ionizing irradiation is known to acutely increase the expression of VCAM-1, ICAM-1, E-selectin, and P-selectin in in vitro cultures of endothelial cells, tumor cells, and in tissue immediately after irradiation [44-45]. In the present report, we demonstrated that pulmonary endothelial cells explanted to culture and irradiated in vitro demonstrated increased acute VCAM-1 activity and that this increase could be reduced by HA-MnSOD transfection prior to irradiation. The late increase in VCAM-1– and ICAM-1–positive endothelial cells in the irradiated lung represents a potentially valuable observation, because the effect followed a latent period of nearly 100 days after whole lung irradiation.

Whether in vivo administration of HA-MnSOD-PL by IT injection facilitated enough deposition of the MnSOD transgene in endothelial cells to be radioprotective and whether the effect of up-regulation of VCAM-1 at the same late time points was also influenced by MnSOD-PL overexpression are not known. Furthermore, it is not known whether those cells with acute up-regulation of VCAM-1 activity after 20 Gy irradiation are the same cells showing increased up-regulation at 100 to 120 days. Because the BrdU labeling studies investigated the day 80 and day 100 time points, and because there were low but detectable levels of increased BrdU at day 80 (although not specifically localized to endothelial cells), it is possible that between days 100 and 120 there was significant turnover of endothelial cells, perhaps the same cells that showed VCAM-1 up-regulation. Further studies in progress, looking at endothelial cells during these intermediate time points between days 80 and 120, should resolve this question.

Irradiation of explanted mouse pulmonary endothelial cells in culture showed that a fraction of these endothelial cells had increased VCAM-1 expression. Whether these were cycling cells is not known. Cell cycle synchronization experiments in progress should resolve this question. It is possible that if VCAM-1 is up-regulated in irradiated cells that go through a cell cycle, and if further experiments demonstrate that between the day 80 and day 120 time points there is a cycling of endothelial cells, the experimental paradigm could reveal that late endothelial cell cycling mediates events that are critical to late pulmonary radiation damage.

Other questions include the following: (1) Which cells in the lung produce the late peak of TGFβ1-β2 detected after day 100 following 20 Gy irradiation? (2) It is known that VCAM-1 up-regulation stimulates monocyte adhesion; therefore, do VCAM-1–up-regulated endothelial cells actively recruit monocytes to the lung to become BAMs, or does passive adherence of naturally circulating monocytes lead to increased monocyte accumulation? It is also not known whether TGFβ1-β2 is produced by BAMs. Other studies from our laboratory demonstrate that irradiated endothelial and bronchoalveolar cells, as well as macrophages, can up-regulate TGFβ1-β2. The significant peak increase in messenger RNA levels for TGFβ1-β2 suggests that a large number of cells are involved in this up-regulation [38]. Studies localizing the TGFβ1-β2 increase to specific cells in the irradiated lung are in progress.

Finally, a question remains regarding the source of proliferating fibroblasts forming the lesions in pulmonary fibrosis. Pulmonary fibrosis in irradiation damage could be caused by resident fibroblasts recruited by TGFβ1-β2 to proliferate and form the fibrotic lesions. The distal site of the fibrotic lesions in the peripheral lung revealed that accumulation of macrophages is also evident, and these cells may induce migration or proliferation of fibroblasts. Alternatively, fibroblast progenitor cells, perhaps from the bone marrow, could also arrive after day 80 to the irradiated lung via the circulation. Recent data from our laboratory support this latter mechanism [56].

The present studies demonstrate that the C57BL/6NHsd mouse model is a valuable system with which to analyze the molecular and cellular events involved in late ionizing irradiation damage to the lung. Further studies should elaborate the cellular and molecular mechanisms of this significant complication of total body irradiation.

ACKNOWLEDGMENT

This work was sponsored by the National Institutes of Health, contract grant no. RO1-HL60132.

REFERENCES

1. Rosenzweig KE, Mychalczak B, Fuks Z, et al. Final report of the 70.2 Gy and 75.6 Gy dose levels of phase I dose escalation study using 3-dimensional conformal radiotherapy in the treatment of NSCLC. *Cancer J.* 2000;6:82-87.
2. Robnett TJ, Machtay M, Vines EF, McKenna MG, Algazy KM, McKenna WG. Factors predicting severe radiation pneumonitis in patients receiving definitive chemoradiation for lung cancer. *Int J Radiat Oncol Biol Phys.* 2000;48:89-94.
3. Sunyach M-P, Falchero L, Pommier P, et al. Prospective evaluation of early lung toxicity following 3-dimensional conformal radiation therapy in NSCLC: preliminary results. *Int J Radiat Oncol Biol Phys.* 2000;48:459-463.
4. Theuws JCM, Seppenwoolde Y, Kwa SLS, et al. Changes in local pulmonary injury up to 48 months after irradiation for lymphoma and breast cancer. *Int J Radiat Oncol Biol Phys.* 2000;47:1201-1208.
5. Martin M, Lefaix J-L, Delanian S. TGFβ1 and radiation fibrosis: a master switch and a specific therapeutic target? *Int J Radiat Oncol Biol Phys.* 2000;47:277-290.
6. Cooper JAD Jr. Pulmonary fibrosis: pathways are slowly coming into light. *Am J Respir Cell Mol Biol.* 2000;22:520-523.

7. Hocher B, Schwarz A, Fagan KA, et al. Pulmonary fibrosis and chronic lung inflammation in ET-1 transgenic mice. *Am J Respir Cell Mol Biol.* 2000;23:19-26.
8. Hall E. *Radiobiology for the Radiologist*. 4th ed. Philadelphia, Pa: JB Lippincott Inc; 1999.
9. Rubin P, Casarett GW. *Clinical Radiation Pathology*. Philadelphia, Pa: WB Saunders; 1968.
10. Geara FB, Komaki R, Tucker SL, Travis EL, Cox JD. Factors influencing the development of lung fibrosis after chemoradiation for small cell carcinoma of the lung: evidence for inherent individual variation. *Int J Radiat Oncol Biol Phys.* 1998;42:279-286.
11. Mah K, Keane TJ, Van Dyk J, Braban LE, Poon PY, Hao Y. Quantitative effect of combined chemotherapy and fractionated radiotherapy on the incidence of radiation-induced lung damage: a prospective clinical study. *Int J Radiat Oncol Biol Phys.* 1994;28: 563-574.
12. Marks LB, Munley MT, Bentel GC, et al. Physical and biological predictors of changes in whole-lung function following thoracic irradiation. *Int J Radiat Oncol Biol Phys.* 1999;89:563-570.
13. Folz RJ. Mechanisms of lung injury after bone marrow transplantation. *Am J Respir Cell Mol Biol.* 1999;20:1097-1099.
14. Shankar G, Bryson JS, Jennings CD, Kaplan AM, Cohen DA. Idiopathic pneumonia syndrome after allogeneic bone marrow transplantation in mice. Role of pretransplant radiation conditioning. *Am J Respir Cell Mol Biol.* 1999;20:1116-1124.
15. Tager AM, Luster AD, Leary CP, et al. Accessory cells with immunophenotypic and functional features of monocyte-derived dendritic cells are recruited to the lung during pulmonary inflammation. *J Leuk Biol.* 1999;66:901-908.
16. Nakada-Tsukui K, Watanabe N, Kobayashi Y. Regulation of the processing and release of TNFα in a human macrophage cell line. *J Leuk Biol.* 1999;66:968-973.
17. Raychaudhuri B, Dweik R, Connors MJ, et al. Nitric oxide blocks NFκB activation in alveolar macrophages. *Am J Respir Cell Mol Biol.* 1999;21:311-316.
18. Gibbs DF, Shanley TP, Warner RL, Murphy HS, Varani J, Johnson KJ. Role of matrix metalloproteinases in models of macrophage-dependent acute lung injury. *Am J Respir Cell Mol Biol.* 1999;20:1145-1154.
19. Gibbs DF, Warner RL, Weiss SJ, Johnson KJ, Variani J. Characterization of matrix metalloproteinases produced by rat alveolar macrophages. *Am J Respir Cell Mol Biol.* 1999;20:1136-1144.
20. Imrich A, Ning Y, Kobzik L. Intracellular oxidant production and cytokine responses in lung macrophages: evaluation of fluorescent probes. *J Leuk Biol.* 1999;65:499-507.
21. Wiley JA, Harmsen AG. Bone marrow-derived cells are required for the induction of a pulmonary inflammatory response mediated by CD40 ligation. *Am J Path.* 1999;154:919-926.
22. Lentsch AB, Czermak BJ, Bless NM, Van Rooijen N, Ward PA. Essential role of alveolar macrophages in intrapulmonary activation of NFκB. *Am J Respir Cell Mol Biol.* 1999;20:692-698.
23. Salez L, Singer M, Balloy V, Creminon C, Chignard M. Lack of IL-10 synthesis by murine alveolar macrophages upon lipopolysaccharide exposure. Comparison with peritoneal macrophages. *J Leuk Biol.* 2000;67:545-552.
24. Wang J, Snider DP, Hewlett BR, et al. Transgenic expression of GM-CSF induces the differentiation and activation of a novel dendritic cell population in the lung. *Blood.* 2000;96:2337-2345.
25. Vancheri C, Sortino MA, Tomaselli V, et al. Different expression of TNFα receptors and prostaglandin E2 production in normal and fibrotic lung fibroblasts. Potential implications for the evolution of the inflammatory process. *Am J Respir Cell Mol Biol.* 2000;22:628-634.
26. Adler H, Beland JL, Kozlow W, Del-Pan NC, Kobzik L, Rimm IJ. A role for TGFβ1 in the increased pneumonitis in murine allogeneic bone marrow transplant recipients with graft versus-host disease after pulmonary herpes simplex virus type I infection. *Blood.* 1998;92:2581-2589.
27. Johnston CJ, Piedboeuf B, Baggs R, Rubin P, Finkelstein JN. Differences in correlation of mRNA gene expression in mice sensitive and resistant to radiation-induced pulmonary fibrosis. *Radiat Res.* 1995;142:197-203.
28. Rubin P, Johnston CJ, Williams JP, McDonald S, Finkelstein JN. A perpetual cascade of cytokines post-irradiation leads to pulmonary fibrosis. *Int J Radiat Oncol Biol Phys.* 1995;33:99-109.
29. Johnston CJ, Piedboeuf B, Rubin P, Williams JP, Baggs R, Finkelstein JN. Early and persistent alterations in the expression of IL-1α, IL-1β, and TNFα mRNA levels in fibrosis resistant and sensitive mice after thoracic irradiation. *Radiat Res.* 1996;145: 762-767.
30. Anscher MS, King FM, Andrews K, et al. Plasma TGFβ1 as a predictor of radiation pneumonitis. *Int J Radiat Oncol Biol Phys.* 1998;41:1029-1035.
31. Blobe GC, Schiemann WP, Lodish HF. Role of TGFβ in human disease. *N Engl J Med.* 2000;87:1350-1355.
32. Sime PJ, Marr RA, Gauldie D, et al. Transfer of TNFα to rat lung induces severe pulmonary inflammation and patchy interstitial fibrogenesis with induction of TGFβ1 and myofibroblasts. *Am J Path.* 1998;153:825-832.
33. Thrall RS, Vogel SN, Evans R, Shultz LD. Role of TNFα in the spontaneous development of pulmonary fibrosis in viable motheaten mutant mice. *Am J Path.* 997;151:1303-1310.
34. Munger JS, Huang X, Kawakatsu H, et al. The integrin alpha v beta 6 binds and activates latent TGFβ1: a mechanism for regulating pulmonary inflammation and fibrosis. *Cell.* 1999;96: 319-328.
35. Hallahan De, Virudachalam S. Intercellular adhesion molecule-1 knockout abrogates radiation induced pulmonary inflammation. *Proc Natl Acad Sci U S A.* 1997;94:6432-6437.
36. Wong GHW. Protective roles of cytokines against radiation: induction of mitochondrial MnSOD. *Biochim Biophys Acta.* 1995;1271:205-209.
37. Epperly MW, Epstein CJ, Travis EL, Greenberger JS. Decreased pulmonary radiation resistance of manganese superoxide dismutase (MnSOD)-deficient mice is corrected by human manganese superoxide dismutase-plasmid/liposome (*SOD2*-PL) intratracheal gene therapy. *Radiat Res.* 2000;154:365-374.
38. Epperly MW, Travis EL, Sikora C, Greenberger JS. Manganese (correction of Magnesium) superoxide dismutase (MnSOD) plasmid/liposome pulmonary radioprotective gene therapy: modulation of irradiation-induced mRNA for IL-1, TNFα, and TGFβ correlates with delay of organizing alveolitis/fibrosis. *Biol Blood Marrow Transplant.* 1999;5:204-214.
39. Epperly MW, Bray JA, Krager S, et al. Intratracheal injection of adenovirus containing the human MnSOD transgene protects athymic nude mice from irradiation-induced organizing alveolitis. *Int J Radiat Oncol Biol Phys.* 1999;43:169-181.
40. Epperly, MW, Bray JA, Kraeger S, et al. Prevention of late effects of irradiation lung damage by manganese superoxide dismutase gene therapy. *Gene Ther.* 1998;5:196-208.
41. Epperly MW, Defilippi S, Sikora C, Gretton J, Kalend K, Greenberger JS. Intratracheal injection of manganese superoxide dismu-

tase (MnSOD) plasmid/liposomes protects normal lung but not orthotopic tumors from irradiation. *Gene Ther.* 2000;7:1011-1018.
42. Franko AJ, Sharplin J. Development of fibrosis after lung irradiation in relation to inflammation and lung function in a mouse strain prone to fibrosis. *Radiat Res.* 1994;140:347-355.
43. Dileto C, Travis EL. Fibroblast radiosensitivity in vitro and lung fibrosis *in vivo*: comparison between a fibrosis-prone and fibrosis-resistant mouse strain. *Radiat Res.* 1996;146:61-67.
44. Hallahan DE, Kuchibhotla J, Wyble C. Sialyl Lewis X mimetics attenuate E-selectin-mediated adhesion of leukocytes to irradiated human endothelial cells. *Radiat Res.* 1997;147:41-47.
45. Quarmby S, Kumar P, Kumar S. Radiation-induced normal tissue injury: role of adhesion molecules in leukocyte-endothelial cell interactions. *Cancer.* 1999;82:385-395.
46. Huaux F, Lardot C, Arras M, et al. Lung fibrosis induced by silica particles in NMRI mice is associated with an up-regulation of the p40 subunit of IL-12 and Th-2 manifestations. *Am J Respir Cell Mol Biol.* 1999;20:561-572.
47. Avila JJ, Lympany PA, Pantelidis P, Welsh KI, Black CM, Du Bois RM. Fibronectin gene polymorphisms associated with fibrosing alveolitis in systemic sclerosis. *Am J Respir Cell Mol Biol.* 1999; 20:106-112.
48. Shang T, Yednock T, Issekutz AC. alpha9beta1 integrin is expressed on human neutrophils and contributes to neutrophil migration through human lung and synovial fibroblast barriers. *J Leukoc Biol.* 1999;66:809-816.
49. Epperly MW, Bray JA, Esocobar P, Bigbee WL, Watkins S, Greenberger JS. Overexpression of the human MnSOD transgene in subclones of murine hematopoietic progenitor cell line 32D cl 3 decreases irradiation-induced apoptosis but does not alter G2/M or G1/S phase cell cycle arrest. *Radiat Oncol Invest.* 1999;7:331-342.
50. Fleming T, Harrington D. A class of hypothesis tests for one and two sample censored survival data. *Commun Stat Theor Methods.* 1981;A10:763-794.
51. Harrington D, Fleming T. A class of rank test procedures for censored survival data. *Biometrika.* 1982;69:553-566.
52. Motulsky H. *Intuitive Biostatistics*. New York, NY: Oxford University Press; 1995:207-213.
53. Holland M, Wolfe D. *Nonparametric Statistical Methods*. New York, NY: John Wiley and Sons; 1973.
54. Epperly MW, Travis EL, Whitsett JA, Epstein CJ, Greenberger JS. Overexpression of manganese superoxide dismutase (MnSOD) in whole lung or alveolar type II (AT-II) cells of MnSOD transgenic mice does not provide intrinsic lung irradiation protection. *Radiat Oncol Invest.* 2001;96:11-21.
55. Epperly MW, Gretton JA, DeFilippi SJ, et al. Modulation of radiation-induced cytokine elevation associated with esophagitis and esophageal stricture by manganese superoxide dismutase-plasmid/liposome (*SOD*-PL) gene therapy. *Radiat Res.* 2001;155:2-14.
56. Greenberger JS, Sikora CA, DeFilippi SJ, Gretton JE, Epperly MW. Bone marrow stromal cell involvement in irradiation pulmonary fibrosis [abstract]. *Exp Hematol.* 2001;29(suppl 1):86.